ENVIRONMENTAL RESEARCH
COMMUNICATIONS

INCLUSIVE PUBLISHING
TRUSTED SCIENCE

Part of the
ENVIRONMENTAL RESEARCH
SERIES

PURPOSE-LED
PUBLISHING™

LETTER • OPEN ACCESS

Variability in quantifying leaf area index in humid, fire-affected ecosystems

To cite this article: N K Corak *et al* 2026 *Environ. Res. Commun.* **8** 051005

Environmental Research Communications

OPEN ACCESS

RECEIVED
19 September 2025

REVISED
7 April 2026

ACCEPTED FOR PUBLICATION
22 April 2026

PUBLISHED
6 May 2026

LETTER

Variability in quantifying leaf area index in humid, fire-affected ecosystems

N K Corak[1,2], S J Kim-Shapiro[1,3], K T Chiarieri[1] and L E L Lowman[1,2,*]

[1] Department of Engineering, Wake Forest University, Winston-Salem, NC, United States of America
[2] Department of Physics, Wake Forest University, Winston-Salem, NC, United States of America
[3] Department of Earth and Planetary Sciences, University of California Santa Cruz, Santa Cruz, CA, United States of America
[*] Author to whom any correspondence should be addressed.

E-mail: lowmanle@wfu.edu

Keywords: prescribed fire, remote sensing, leaf area index, vegetation regrowth

Abstract

Despite the prevalence of fire activity in the Southeastern United States, a limited understanding of how vegetation phenology varies after fire across different ecosystems hinders our ability to make informed land management decisions and to model vegetation responses at regional scales. Quantifying variability in post-fire observations of canopy structure is essential for land managers assessing damage and recovery, and for ecosystem modelers evaluating changes in carbon uptake, plant water use, and energetic exchanges between the land surface and the atmosphere. Land managers and scientists frequently rely on satellite remote sensing to evaluate vegetation changes in response to fire disturbances. However, satellite remote sensing data are limited by their spatial and temporal resolutions, possibly missing small fires or not capturing heterogeneous impacts to vegetation within a single pixel. To assess this gap, we quantify differences in remote sensing and ground observations of vegetation phenology, evaluating and attributing sources of uncertainty for gridded datasets typically used at ecosystem scales. We quantify phenologic changes across different ecoregions in North Carolina, USA using time series of plant density from ground observations and satellite remote sensing. Using leaf area index (LAI) as a measure of canopy structure, we evaluate changes in vegetation across different fire-affected ecosystems. Based on nearly 400 ground-based measurements collected over a 4-year span before and after prescribed fires and one wildfire, we quantify discrepancies in LAI among satellite and ground products and show how uncertainty varies with ecoregion, plant functional type, spatial resolution, and sub-pixel vegetation heterogeneity. We find that while the magnitudes of LAI estimates differ across data products, seasonal cycles before and after fire events tend to agree. Our results underscore the importance of targeted ground-validation efforts and offer practical insights for improving remote sensing based assessments of post-disturbance vegetation dynamics, carbon and water cycling, and land management.

1. Introduction

The vegetated land surface is the most uncertain component of the carbon budget in future projections [1], and vegetation responses to disturbances like fire are a key component of that uncertainty [2, 3]. Leaf area index (LAI) is an essential parameter used in Earth system modeling that often comes from satellite remote sensing [4, 5]. LAI is a measure of canopy density, defined as the one-sided leaf area per unit ground area [6]. In hydrological modeling, LAI represents the amount of vegetation in simulations of biophysical processes that estimate carbon and water fluxes between the land surface and atmosphere [5, 7]. LAI is often used to evaluate structural and phenologic changes at ecosystem scales in response to extreme events like fire [8–11]. Uncertainty in estimates of LAI from remote sensing products [12] can propagate through land surface models [13], impacting numerical weather prediction [14, 15], estimates of crop production [16–18], and assessments of photosynthetic contributions to evapotranspiration

and carbon assimilation [4, 5, 19, 20]. Thus, it is critical to understand the sources of uncertainty that contribute to estimates of LAI.

Disturbances such as fire alter vegetation structure and subsequently influence carbon and water fluxes [21–23]. In fire-dependent ecosystems, such as longleaf pine savannas in the Southeastern United States, regular, low-intensity fires maintain open canopies that promote understory biodiversity and help sustain carbon cycling regimes [24–28]. Fire frequency and intensity control recovery dynamics and resilience [29, 30], but over the last four decades both have increased due to a combination of climate change and fire suppression [2, 31], amplifying uncertainty in regional carbon cycling [24]. However, a gap remains in understanding how variability in post-fire vegetation phenology propagates to estimates of ecosystem water use and photosynthesis. Thus, quantifying the uncertainty of fire effects on vegetation phenology is paramount to improving estimates of carbon, energy, and water fluxes between Earth's surface and atmosphere.

The impacts of fire on canopy structure can be evaluated through observations of surface properties using satellite imagery [32, 33]. While remote sensing of land surface reflectances can be used to monitor post-fire phenological changes [34], indices such as normalized vegetation difference index (NDVI, a measure of vegetation greenness) can be susceptible to saturation, reflecting rapid recovery [35], or exhibit variability in response rate due to vegetation heterogeneity not captured by satellites [36]. In the Southeast US where NDVI saturates at low values (i.e. the relationship between the vegetation index and spectral reflectance breaks down), LAI can provide an improved estimate of vegetation phenology [37, 38]. To quantify post-fire vegetation regrowth, most studies use vegetation indices derived from satellite remote sensing [9, 34, 39–41], with some using *in situ* observations to capture canopy structure and density [42–44]. While LAI is typically derived from remote sensing observations for modeling, it may also be estimated through direct and indirect field measurements [4, 5, 7].

Indirect optical techniques such as the canopy gap fraction method [45–47] can be employed with handheld devices as a non-invasive way to measure LAI on the ground after fires. Flerchinger *et al* [42] used a combination of the gap fraction method with biomass sampling to estimate annual vegetation recovery and subsequent hydrological impacts following prescribed fire in a semi-arid sagebrush rangeland in southwestern Idaho. Gričar *et al* [43] performed more frequent measurements of LAI (every 7–10 d) to capture spring sprouting of *Q. pubescens* for two months of spring after a wildfire in southwestern Slovenia showing the effects of fire on carbon and water balances and ultimately growth and development patterns. These studies underscore the value of high-frequency, ground-based LAI measurements for evaluating post-fire ecosystem response, while highlighting the critical need for longer-term *in situ* observations to calibrate and validate satellite-derived LAI and capture vegetation regrowth trajectories over time and across diverse fire-adapted ecosystems [41]. Leveraging both satellite-derived and ground-based observations of LAI, we examine how spatial and temporal scale differences, and their associated uncertainties [48], influence assessments of post-fire vegetation recovery.

As prescribed fires and wildfires occur frequently in the Southeastern US, there is a rich body of fire-related literature in the region that focuses on historical fire regimes and land management practices [28, 49], species richness and diversity [50], and the uncertainty of climate change altering the intensity, frequency, and impacts of fire [24]. However, there has been less focus on evaluating how frequent fire disturbances in this region influence measurements and observations of vegetation phenology. Van Leeuwen [39] used satellite-derived NDVI to understand how treatments like prescribed fire can build resilience to wildfires in Arizona. Lacouture *et al* [40] leveraged NDVI to track recovery in a sandy pine forest in Florida following prescribed fire, but those results were limited by growing season cloudiness and lack of *in situ* observations, suggesting future studies incorporate ground-based methods to account for vegetation heterogeneity. Thus, a gap exists in quantifying uncertainty in vegetation phenology for humid, fire-adapted regions like the Southeastern US.

The goal of this study is to quantify variability among satellite and ground observations of vegetation density in fire-affected ecosystems to inform Earth system models that seek to accurately capture land surface fluxes. We hypothesize that the uncertainty in estimates of vegetation phenology in fire-affected regions, as measured by LAI, varies systematically across data collection methods (satellite versus ground observation), physiographic region, and plant functional type. Moreover, we hypothesize that differences between satellite remote sensing and ground observations of LAI will vary according to spatial resolution of the satellite product [51] and sub-pixel vegetation heterogeneity [52]. This study examines vegetation regrowth dynamics following prescribed fire across multiple ecosystems in the North Carolina (NC) Piedmont and Coastal Plains physiographic regions. Over four years, we collected nearly 400 ground-based observations across fifteen sites affected by more than a dozen prescribed fires and one wildfire,

capturing monthly to seasonal changes in LAI. These data support cross-validation of multiple satellite-derived vegetation products and help identify drivers of uncertainty in observations of regrowth dynamics. Insights gained will strengthen global remote sensing applications for vegetation monitoring programs, with broad implications for post-disturbance ecosystem modeling and practical land management decisions.

2. Methods and data

2.1. Overview

The goal of this study was to quantify uncertainty in estimates of vegetation phenology for fire-affected ecosystems across NC. We selected sites in collaboration with the NC Wildlife Resources Commission (NCWRC), the NC Forest Service, and The Nature Conservancy that represent important ecoregions in NC and ensured that the sites were aligned to cross gradients of topography and subsurface properties. We collected satellite remote sensing and ground-based observations of LAI from January 2021 to January 2025 across 15 sites, within 13 burn units, spanning five study areas of grasslands, forests, and savannas in the NC Piedmont and Coastal Plains physiographic regions (figures 1 and 2). Satellite remote-sensing estimates of LAI were derived from the Moderate Resolution Imaging Spectroradiometer (MODIS) and Landsat, while ground observations were obtained using a LICOR LAI-2200 plant canopy analyzer (see sections 2.3 and 2.4). Burn unit boundaries were defined by land managers, while the research team deliberately selected ground-observation locations within spatially uniform areas and away from boundaries to ensure that measurements were representative of the dominant vegetation. Locations and site descriptions are provided in tables 1 and 2. Preliminary data were also collected in the Blue Ridge physiographic region of the NC mountains, but data collection was halted as a result of damage from Hurricane Helene in September 2024. No prescribed fires occurred at this site during the study and no analyses were performed, but the few collected data are included in published datasets.

2.2. NC study sites

2.2.1. Piedmont grassland

The two burn units at Grissom (GR) Field, Main (GR-Main) and Volunteer (GR-Vol), are located on private land in the Central Piedmont of NC. The sites have been managed since 2006 to maintain native grasses that improve wildlife habitat for non-game species. GR-Main is approximately 5 ha and contains primarily big bluestem (*Andropogan gerardii*) with some blackberry (*Rubus spp.*) and goldenrod (*Solidago rigida*). GR-Main was first burned in 2007, followed by the planting of the native grasses, and has been subject to annual prescribed fires in late winter or early spring since 2014. GR-Vol is a 7 ha site of mixed grasses and diverse forbs, first burned in 2015 and left to regrow naturally from the existing, 'volunteer' seed bank. We collected monthly ground measurements of LAI at GR from April 2021 to December 2024.

Reynolda Meadow (RM) is a 3 ha grassland maintained on the grounds of Reynolda Gardens and managed by Wake Forest University in Winston-Salem, NC. Unlike other properties in this study, Reynolda Meadow is situated in a suburban area. A restoration project of the meadow began in 2012 to restore a natural Carolina Piedmont prairie. After mowing and herbicidal treatments, land managers planted a variety of native grasses and forbs. The meadow is mowed or burned annually to replicate the natural burn cycle of Piedmont prairies. In January 2021, we began collecting ground records of LAI at three locations within the boundary, the northwest corner (RM-NW), the southeast corner (RM-SE), and a location in the middle of the field where a small tower (RM-TW) was set up to take temperature readings during a prescribed burn. The only fire at RM during the study period occurred on February 15, 2024.

2.2.2. Piedmont forest

The Falls Lake site in northern Wake County, NC, is game land managed by the NCWRC. The 23 ha burn unit is composed primarily of natural loblolly pine (*Pinus taeda*) overstory and a shrubby understory. Prescribed fire is implemented every two to three years as a strategy to thin the understory for wildlife corridors and to maintain visibility for hunting. During the study period, there were two prescribed fires: March 22, 2022 and April 2, 2024. We took ground-based measurements of LAI before and after each burn.

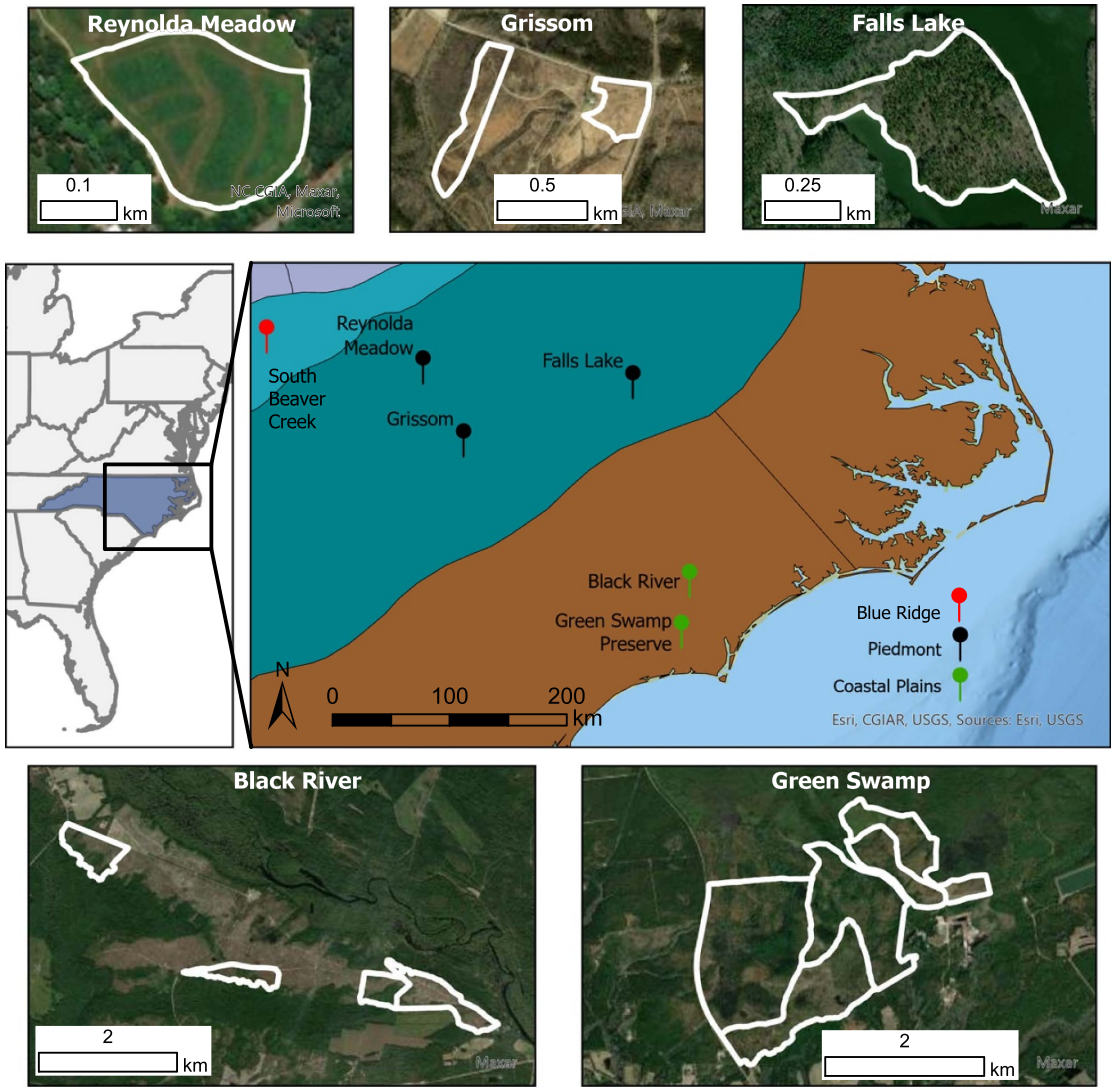

Figure 1. Maps of the five study areas across different North Carolina physiographic regions (Teal = Piedmont, Brown = Coastal Plains). White outlines in border figures indicate burn units for prescribed fires. South Beaver Creek, in the Blue Ridge Mountain region of North Carolina is indicated on the map, though data collection at this site was halted by Hurricane Helene in 2024 and not included in the analysis in this manuscript.

2.2.3. Coastal plains

The Nature Conservancy of NC manages two large preserves in the Southeastern Coastal Plains: the Black River (BR) Preserve, covering over 1600 ha in southeastern Bladen County, and the Green Swamp (GS) Preserve, located about 45 km south, spanning more than 6500 ha. Prior to current land management, the area was used for agricultural purposes. There is evidence of historical fire regimes in each preserve [53–56]. Currently, prescribed fire is used to mimic historical return intervals to restore the natural ecosystem, maintain lands for recreation, and preserve rare and endangered species such as the bald cypress (*Taxodium distichum*) and Venus flytrap (*Dionaea muscipula*). The ecosystems in the preserves consist of upland longleaf pine (*Pinus palustris*) savannas and flatwoods, with wire-grass (*Aristida stricta*) understories, and lowland pocosin and pond pine (*Pinus serotina*) woodlands and shrublands. Regions with longleaf pine are burned with intervals every two to four years which is more frequent than the pocosin wetlands where prescribed fire occurs every five to twenty years. Burn intervals vary based on need, location, complexity, and resource availability.

There are four burn units at BR (Crane A, BR-CA; Lewis B, BR-LB; Lewis D, BR-LD; and Bucher, BR-B) and five burn units at the GS (Clemmons A, GS-CA; Clemmons B, GS-CB; Meyers 1, GS-M1; Meyers 2, GS-M2; and Meyers 3, GS-M3). Data collection at each location began in July 2022 and ended in January 2025. There was a wildfire that affected most of the GS in June 2023, halting plans for prescribed fires at GS-CA, GS-M1, and GS-M2. See tables 1 and 2 for summary descriptions of the sites.

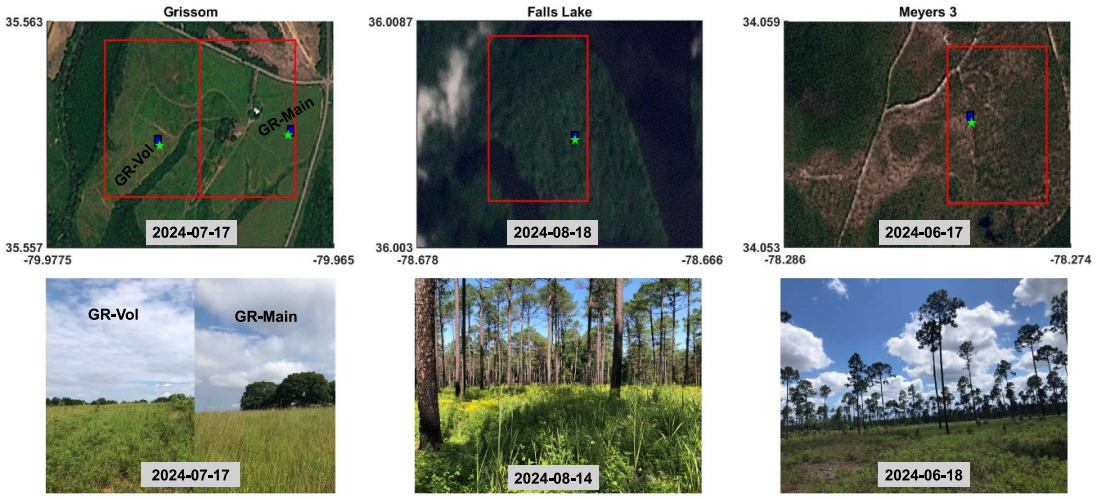

Figure 2. (top row) Aerial views of sites with MODIS (500 m, red outline) and Landsat (30 m, blue boxes) pixels containing locations of ground observations (green star) for Piedmont Grassland (Grissom, Main and Volunteer), Piedmont Forest (Falls Lake) and Coastal Plains (Green Swamp Meyers 3). (bottom row) Ground photos of vegetation from data collection (dates marked on photos). Imagery © 2026 Planet Labs www.planet.com.

Table 1. Study site locations, burn dates, and burn frequencies (RM = Reynolda Meadow; GR = Grissom; BR = Black River; GS = Green Swamp).

Site name	Lat	Lon	Area (ha.)	Burn date(s)	First collection	Frequency
GR-Main	35.560	−79.967	5	2021-03-12, 2022-04-04, 2023-03-22, 2024-02-29	2021-03-12	monthly
GR-Vol	35.559	−79.973	8	2021-03-12, 2023-12-23	2021-03-12	monthly
RM-NW	36.120	−80.279				
RM-TW	36.120	−80.278	3	2024-02-15	2021-01-15	monthly
RM-SE	36.120	−80.277				
Falls Lake	36.006	−78.671	23	2022-03-22, 2024-04-02	2022-03-22	2-3 months
BR-Bucher	34.483	−78.218	35	2023-05-12, 2023-08-03	2022-07-15	2-3 months
BR-CraneA	34.497	−78.259	16	2024-02-03	2022-07-15	2-3 months
BR-LewisB	34.483	−78.237	17	2022-07-20	2022-07-15	2-3 months
BR-LewisD	34.482	−78.223	26	2022-07-20	2022-09-05	
GS-ClemmonsA	34.069	−78.270	46	*2023-06-14	2022-09-05	2-3 months
GS-ClemmonsB	34.068	−78.273	31	2022-07-05,*2023-06-14	2022-07-15	2-3 months
GS-Meyers1	34.051	−78.290	153	*2023-06-14	2022-09-05	2-3 months
GS-Meyers2	34.061	−78.275	95	*2023-06-14	2022-09-05	2-3 months
GS-Meyers3	34.056	−78.278	79	2022-07-06,*2023-06-14	2022-07-15	2-3 months

* denotes the ignition date of a wildfire in the Green Swamp.

2.3. Ground observations

Ground-based LAI was measured using the LAI-2200 C Plant Canopy Analyzer (LI-COR Inc. Lincoln, Nebraska, USA). The device uses the canopy gap fraction method [5, 57, 58] to estimate LAI by measuring the amount of incoming solar radiation above and below the canopy at five angles from the zenith [59]. Open sky, or above canopy, readings provide a baseline for total incoming radiation, while the below canopy reading measures how much light passes through the canopy. A 180° lens cap was used when taking below canopy (ground measurements) to block the sensor operator. Above canopy measurements were taken above the grasses and in open sky patches adjacent to the burn units for taller canopies. Below canopy observations attempted to capture all aboveground vegetation by placing the optical sensor on the ground. The computations performed on the accompanying LAI-2270 console estimate LAI based on the probabilities that light will pass through the canopy at the five mask angles while accounting for clumping and foliage orientation.

Table 2. Land cover classifications and site descriptions.

Site name	MCD12Q1 Type 3	NLCD 2021	Land management descriptions
GR-Main	Savanna	Pasture/Hay	Planted grassland dominated by big bluestem (*A. gerardii*)
GR-Vol	Savanna	Pasture/Hay	Mixed native grasses (*A. virginicus*, *P. anceps*) and a wide variety of forbs
RM-NW	Savanna	Pasture/Hay	Mixed grassland with big bluestem (*A. gerardii*) and switchgrass (*P. vergatum*)
RM-TW	Savanna	Pasture/Hay	Some forbs milkweed (*A. syriaca*) and goldenrod (*S. rigida*)
RM-SE	Savanna	Deciduous forest	
Falls Lake	Deciduous Broadleaf Forest	Evergreen forest	Loblolly pine (*P. taeda*) overstory with a shrubby understory
BR-Bucher	Savanna	Grassland	Longleaf pine Savanna (*P. palustris*) Wiregrass (*A. stricta*) understory and some pocosin.
BR-CraneA	Savanna	Grassland	
BR-LewisB	Savanna	Grassland	
BR-LewisD	Savanna	Grassland	
GS-ClemmonsA	Savanna	Shrubland	Longleaf pine Savanna (*P. palustris*) Wiregrass (*A. stricta*) understory and some pocosin
GS-ClemmonsB	Savanna	Evergreen forest	
GS-Meyers1	Savanna	Evergreen forest	
GS-Meyers2	Savanna	Evergreen forest	
GS-Meyers3	Savanna	Evergreen forest	

Measurement frequency varied by site based on accessibility. Ground measurements were collected monthly at the grassland sites of GR Field and Reynolda Meadow, but at 2–3 month intervals for the remaining sites (table 1). At each site, one above canopy reading and 9–12 below canopy readings were taken within a 10 m grid to capture foliage variability due to stand heterogeneity which are averaged within the handheld console to produce a single LAI estimate. The built-in 'Clip' function on the console was used to correct readings where canopy transmittance was greater than one [59], which primarily occurred at BR-LB, where the canopy is sparse.

2.4. Remote sensing data

2.4.1. MODIS LAI

The MODIS MOD15A2H Version 6.1 Level 4 500 m 8 d LAI [60] were acquired using the NASA Earth Data Application for Extraction and Exploring Analysis Ready Samples (A$\rho\rho$eears, https://appeears.earthdatacloud.nasa.gov/). The main algorithm uses near infrared (858 nm) and red (648 nm) surface reflectances to solve a three-dimensional radiative transfer equation, using lookup tables that associate surface reflectance characteristics with vegetation canopy structure [4, 61], using the best image from the Terra satellite observations over an 8 d composite period. The LAI algorithm estimates vegetation density based on the MCD12Q1 Land Cover Type 3 classification [62], which provides annual, global land cover at a 500 m resolution. Annual MCD12Q1 data were obtained from Appeears.

2.4.2. Landsat-derived LAI

We estimated 30 m LAI using a machine learning algorithm adapted from Kang *et al* [63], implemented in Google Earth Engine (GEE, https://earthengine.google.com/ [64]). Their model used spatially homogeneous samples of MODIS LAI and Landsat 5, 7, and 8 reflectance with separate random forest models for eight NLCD-defined biomes for each sensor. LAI was computed using only Landsat 8 surface reflectance imagery, selected for its improved spectral sensitivity and temporal alignment with the study period [65]. Surface reflectance values outside the training sample's convex hull are flagged and LAI is not produced when excessive clouds are present [63]. The temporal frequency of cloud-free LAI readings is approximately two per month in this study. The 30 m NLCD dataset matches the Landsat resolution and is updated periodically [66]. We extracted NLCD 2021 data [67] using GEE.

2.5. Spatiotemporal alignment of ground and remotely-sensed LAI

To compare point-based ground observations with pixel-based remotely-sensed LAI, we identified the corresponding MODIS and Landsat pixels and temporally interpolated satellite observations so they aligned in both space and time with satellite observations. At GR, the ground observations inside of the two burn units (Main and Volunteer) fall in distinct, adjacent MODIS pixels (figure 2). These observations also fall into separate Landsat pixels. At Reynolda Meadow, the three ground observation sites fall within the same MODIS pixel, but three distinct Landsat pixels. At the GS and BR, burn units are far enough apart that site-level ground observations for each burn unit occur within distinct MODIS and Landsat pixels. In the Piedmont Forest, ground observations were collected at a single location, corresponding to one MODIS pixel and one Landsat pixel.

The MODIS and Landsat-derived LAI products required data processing before being suitable for analysis. We applied a Savitsky–Golay filter [68] following Chen *et al* [69] to smooth noisy measurements associated with nonphysical, rapid changes in remotely sensed LAI due to cloud contamination [70], atmospheric disturbances, or sensor properties [38]. A Savitsky–Golay filter uses least-squares regression to fit a low-degree polynomial over a smoothing window [68, 69], and is commonly used to preserve seasonality in phenology time series [71, 72].

We began by flagging and linearly interpolating LAI values using quality control (QA) bands. For MODIS, we removed values of LAI derived from the NDVI-based backup algorithm [4, 61], which is more prone to cloud contamination [70, 73]. We excluded the NDVI-based LAI estimates due to unreliable performance in areas with non-photosynthetic (dead or brown) vegetation [74]. For Landsat-derived LAI, we used the binary QA flag from Kang *et al* [63] to exclude values of reflectance outside of the range of the training sample. When neighboring pixels experienced similar nonphysical increases in LAI without consistent QA flags, we manually flagged and removed them. This occurred fewer than five times.

We linearly resampled the Landsat data at the highest possible temporal resolution to ensure equal spacing of the data, a necessary condition for the Savitsky–Golay filter [68]. The spacing varied slightly for each site at approximately one-month. We used a polynomial of $d = 4$ and, to ensure the smoothing windows represented comparable time spans, we used a half-window lengths of $m = 4$ for Landsat and $m = 6$ for MODIS, both within the recommended range [69]. Finally, smoothed data were linearly interpolated to a daily time step to align remote sensing data with dates from ground-based measurements for regression analysis.

3. Results and discussion

3.1. Post-fire vegetation regrowth patterns and interannual variability across ecoregions

Vegetation growth after fires and after the dormant season is observed with increases in LAI that tend to peak in mid-summer months across all NC ecoregions. However, the magnitude of peak season LAI varies by observation methods and region (figure 3). These discrepancies in seasonal LAI likely arise from differences in spatial resolution, measurement approach, and land cover classification. Coarse spatial resolution of satellites which may not capture vegetation heterogeneity, lead to mismatches with ground data [73] (figure 2). Biases in ground based-instruments like the LI-COR may overestimate LAI in dense grasslands or underestimate it in sparse canopies such as longleaf pine savannas [5, 58, 75].

Land cover misclassifications further contribute to the differences among observational methods. The MODIS classifications often disagree with the NLCD biome classifications and from land manager descriptions (table 2). Among the 15 locations in this study, there were five different land cover types from NLCD but only two from MODIS, which classified fourteen locations as savannas and one as deciduous broadleaf forest. The coarse resolution of MODIS can lead to misclassifications in heterogeneous landscapes which affect estimates of LAI because LAI algorithms rely on land cover-specific surface reflectance assumptions [76, 77]. In contrast, NLCD differentiates more specific land cover types due to its finer spatial resolution. For example, in Coastal Savannas, MODIS identifies all sites as savannas, but NLCD classifies the BR sites as grasslands and most GS sites as evergreen forests, with the exception of GS-CA (shrubland). Discrepancies in land cover classification, which influence surface reflectance dependence in LAI algorithms, may contribute to differences in LAI across data sources. Further discussion of site- and region-specific results are described in the following subsections.

3.1.1. Piedmont grasslands

Rapid post-fire regrowth was observed at GR Field from 2021 to 2024 (figures 3(a) and (b)). Because fires in Piedmont grasslands, especially those affecting big bluestem, typically occur early in the growing

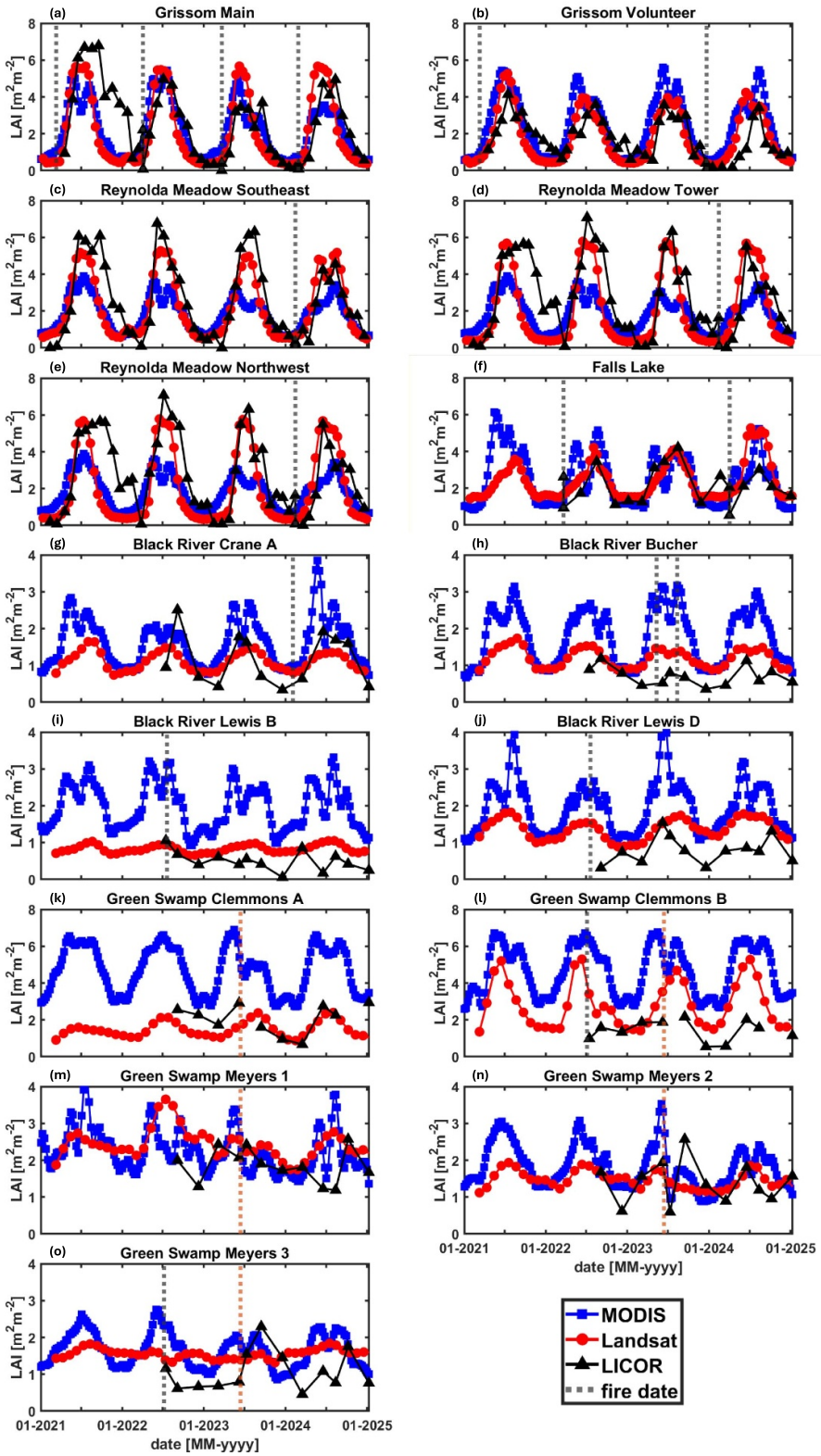

Figure 3. Leaf area index (LAI) from January 2021 to January 2025 from MODIS, Landsat, and LI-COR. Gray dotted lines indicate dates of prescribed fire. In the Green Swamp, wildfire is signified with orange dotted lines.

season, rapid regrowth was likely driven by elevated surface temperatures that amplify photosynthesis [78, 79] or the post-fire resprouting that can occur in frequently burned grassland and savanna ecosystems [80, 81].

Although MODIS (MCD12Q1) classification for GR-Main was savanna instead of grassland, the interannual LAI from MODIS are in seasonal agreement with ground observations (figure 3(a)). All three methods agree seasonally at both GR sites, but differ in peak season LAI. Ground observations

in 2023 were more than 2.0 $m^2 m^{-2}$ below the satellite measurements. In 2024, MODIS LAI is lowest, which could be due to nearby logging within the MODIS pixel (figure 2).

Landsat LAI at GR-Main exceeded 5.5 $m^2 m^{-2}$ in summer, with similar values observed by MODIS from 2021 to 2023. Peak season LAI from ground observations at GR-Main ranged from 3.7 to 6.6 $m^2 m^{-2}$ demonstrating more interannual variability than satellite-derived estimates. Ground observations in 2021 remain high throughout the autumn and early winter as dense, dormant vegetation continued to block light in below canopy readings. At Reynolda Meadow, Landsat shows better agreement with LI-COR measurements, while MODIS LAI values tend to be lower (figures 3(c)–(e)). Rapid regrowth across datasets is largely driven by the timing of dormant or early growing season prescribed fires in the Piedmont Grasslands, which minimally disrupt seasonal LAI dynamics; however, differences in peak LAI reflect sensitivities to measurement method, spatial scale, and land cover misclassifications in these ecosystems.

3.1.2. Piedmont forests

At Falls Lake, ground-based LAI decreased from 2.6 to 0.9 $m^2 m^{-2}$ the morning of the March 2022 prescribed fire (figure 3(f)). By August, ground-based LAI increased to 3.4 $m^2 m^{-2}$ while MODIS and Landsat LAI were 5.1 and 3.9 $m^2 m^{-2}$, respectively. In the summer following the 2024 prescribed fire, ground-based LAI was 3.0 $m^2 m^{-2}$, while MODIS and Landsat LAI were 5.1 and 5.0 $m^2 m^{-2}$, respectively. Higher satellite-derived LAI could be due to the very green nature of the understory in August 2024 at Falls Lake (figure 2), as well as the fact that the ground observations do not directly measure greenness but instead quantify the amount of sunlight blocked by vegetation. The May–June decrease in MODIS LAI in some years is likely an algorithmic artifact associated with high sun angles impacting bidirectional reflectances or rapid canopy changes that induce saturation [4, 5, 61]. Satellite-derived LAI overestimation at Falls Lake is a phenomenon observed in other mature forests, likely resulting from signal saturation [82]. Satellite derived estimates are influenced by chlorophyll content reflecting green light rather than capturing actual density, whereas the canopy gap fraction method captures plant area directly from blocked sunlight. This measurement bias can contribute to systematic discrepancies between the two datasets in this ecosystem and should be accounted for when assessing impacts of fire from satellite observations. While rapid post-fire recovery is also evident in Piedmont Forests, satellite-derived LAI tends to overestimate canopy density due to sensitivity to greenness and saturation, requiring careful interpretation of structural change.

3.1.3. Coastal Savannas

A prescribed fire occurred at GS Meyers 3 on July 6, 2022 and we began collecting ground observations 9 d later. Prior seasonal MODIS LAI ranged from 1.1 and 2.7 $m^2 m^{-2}$ but fell to between 0.9 and 2.3 $m^2 m^{-2}$ after the prescribed fire (figure 3(o)). In contrast, all Landsat LAI values fell between 1.3 and 1.8 $m^2 m^{-2}$, indicating much smaller seasonal variation. The ground-based LAI ranged from 0.5 to 2.3 $m^2 m^{-2}$. Although the range reflects seasonal growth, low summer LAI could be due to the open, clumped nature of the canopy at Meyers 3 (figure 2) which can overestimate the gap fraction and underestimate LAI [58, 83]. Understory grasses may increase the scattering of light and could be the cause of higher LAI measurements [84, 85] in late 2023 and autumn 2024 (figure 3(o)).

Immediately following the prescribed fire, ground-based LAI at GS-M3 remained low until it increased in July and September 2023, shortly after a wildfire burned through the region in June (figure 3(o)). A similar signal was observed in GS-M2 with ground-based LAI over 2 $m^2 m^{-2}$ in September 2023 (figure 3(n)). This post-wildfire increase may reflect enhanced regrowth capabilities of fire-adapted species in longleaf pine savannas [86] and pocosin woodlands [56]. Otherwise, LAI remained stable, suggesting prior prescribed fire may build resilience to wildfire [29, 87, 88]. However, further research is needed to determine if resilience and rapid regrowth holds across the entire GS. In GS areas not burned with prescribed fire in 2022 (GS-CA, GS-M1, GS-M2), the 2023 wildfire caused larger losses to LAI, most of which are observed in the post-fire decreases in MODIS LAI (figures 3(k), (m) and (n)). Accessibility was limited for GS-CA and GS-CB in the few months following the wildfire, but MODIS observed the decline in LAI at both sites. Recovery is seen in all GS burn units with peak LAI in 2024 returning to values similar to those before the wildfire.

Overall, LAI values are lower in the Coastal Savannas (figure 3), with both MODIS and the LI-COR measuring higher maximum LAI than Landsat. In the BR burn units, MODIS LAI is nearly double Landsat and ground-based measurements (figures 3(g)–(j), and the discrepancies with MODIS are even larger in the GS-Clemmons stands (figures 3(k)–(l)). Except at GS-CB, Landsat observes steady, subtle seasonal patterns in LAI with low annual variability. At GS-CB, both MODIS and Landsat observe large

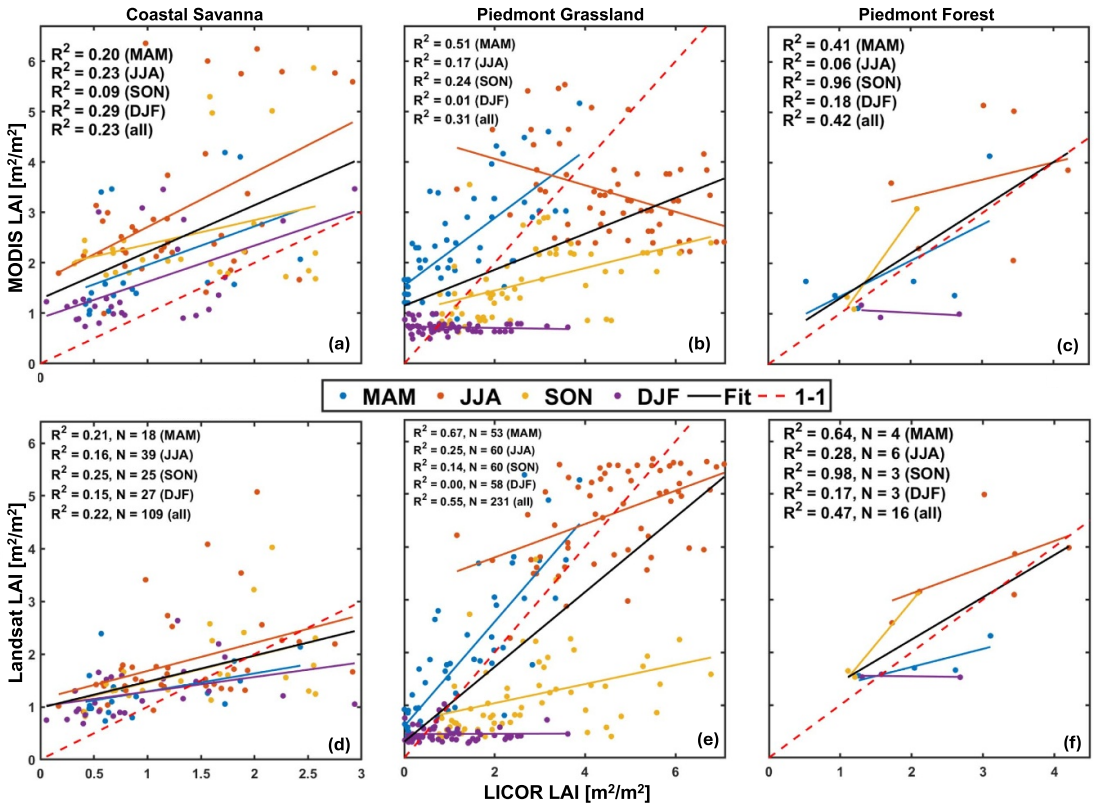

Figure 4. Comparisons of satellite-derived and ground-based measurements of leaf area index (LAI, $m^2\ m^{-2}$) by ecoregions: Coastal Savanna, Piedmont Grassland, Piedmont Forest, with MODIS in the top panels and Landsat in the bottom panels. Coefficients of determination, R^2, are shown by seasons and for all time: spring (MAM = March, April, May); summer (JJA = June, July, August); autumn (SON = September, October, November); and winter (DJF = December, January, February). Red, dashed lines are one-to-one.

interannual fluctuations in LAI, with MODIS ranging from 2.7 to 6.7 $m^2\ m^{-2}$, Landsat ranging from 1.4 to 5.3 $m^2\ m^{-2}$, and ground-based observations oscillating between 0.5 and 2.1 $m^2\ m^{-2}$.

Aside from a few of the extreme values, the LI-COR estimates align with ground-observed LAI captured by hemispherical photography ranging from 0.2 to 1.1 $m^2\ m^{-2}$ across soil moisture gradients in prescribed-fire managed longleaf pine savannas in the Coastal Plains of Georgia [89]. Thus, we caution researchers and land managers using MODIS to estimate peak season LAI in Coastal Savannas as it may overestimate vegetation density. Landsat-derived LAI overestimates ground-based LAI less than MODIS in the Coastal Savannas and maintains a consistent relationship with ground observations across seasons, so incorporating ground observations, finer-resolution remote sensing, or other complementary measurements (e.g. LiDAR [90]) can improve estimates of vegetation density and recovery (figure 4(d)).

3.2. Seasonal variation in satellite-derived and ground-based measurements of LAI

Satellite-derived and ground-based LAI exhibit regional and seasonal variability with large discrepancies across ecoregions (figure 4). MODIS and Landsat align best with ground observations during Piedmont spring where regression slopes are closest to the 1:1 line (red dashed curve in figure 4). In the Piedmont Forest, R^2 is 0.41 for MODIS and 0.64 for Landsat in Spring (figures 4(c) and (f)). In Piedmont Grasslands, performance improves to 0.51 and 0.67 (figures 4(b) and (e)), respectively. In contrast, Coastal Savannas show weaker agreement with $R^2 < 0.23$ for MODIS and 0.22 for Landsat across all seasons (figures 4(a) and (d)). The highest seasonal values of R^2 for MODIS and Landsat in this region are 0.29 for MODIS winter and 0.25 for Landsat autumn though R^2 values are similar across all seasons. The low R^2 values likely result from variability in the number of longleaf pine trees and density of understory vegetation across the nine Coastal Savanna sites. However, at any given site there is consistent vegetation throughout the year whereas the Piedmont sites experience more intra-annual fluctuations driven by seasonal changes in vegetation greenness.

Despite lower R^2 values, Coastal Savannas show more seasonally consistent relationships, especially for Landsat, with consistent slopes across seasons (figure 4(a)). While Landsat fit lines generally match

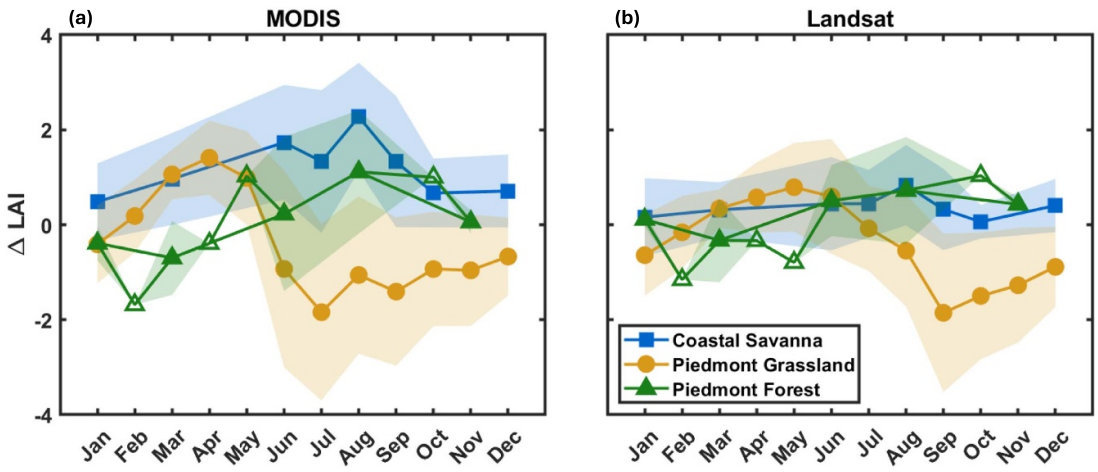

Figure 5. Monthly mean differences between satellite-derived and ground-based LAI. Δ *LAI* = satellite—LI-COR. Shaded regions indicate ± 1 standard deviation for each ecoregion. Results are shown for MODIS (left) and Landsat (right). Open triangles in the Piedmont Forest indicate only one data point for the given month, and thus no standard deviation.

the 1:1 reference, the slopes are less than one, indicating overestimation of low ground-based LAI values and underestimation of high values. MODIS LAI consistently estimates higher values than ground-based measurements, with most data and regression lines above the 1:1 line (figure 4(a)). MODIS likely overestimates LAI compared to the gap fraction method with the LICOR in Coastal Savannas because it interprets strong understory greenness within coarse, heterogeneous pixels as dense canopy structure [4], failing to capture the open, clumped nature of these ecosystems.

In the Piedmont Forests, linear relationships vary considerably across seasons. Despite the variability, some of the highest values of R^2 come from the Piedmont Forest, with an overall $R^2 = 0.42$ for MODIS and 0.47 for Landsat (figures 4(c) and (d)). The two satellite-derived products performed comparably against ground-based measurements with consistent slopes of seasonal regressions, but variability in R^2 can be attributed to the small samples sizes ($N = 17$ for 2022 through 2024). For example, $R^2 \geqslant 0.96$ in autumn for both MODIS and Landsat, but $N = 3$, limiting the reliability of the regression. More sampling is needed in the Piedmont Forest to draw more detailed conclusions about the agreement of ground observations and remote sensing data.

In contrast to the Piedmont Forest and despite having 62 data points in winter for Piedmont Grasslands, low LAI from MODIS and Landsat yield little correlation with ground observations ($R^2 \leqslant 0.01$, figures 4(d) and (e)). The patterns of regression lines in Piedmont Grasslands also shift by season. Autumn and winter fall primarily under the 1:1 line, while spring estimates fall above it and summer lines cross it. Moreover, the regression slope for MODIS summer is negative. Ground-based measurements during summer indicate that the grasslands are covered with dense vegetation (LAI $> 6\,m^2\,m^{-2}$), at times more than double MODIS which is relying on biome specific parameters to interpret surface reflection [4], underscoring the complexity of comparing satellite-derived and ground-based LAI. These seasonal and regional patterns suggest that any efforts to adjust or interpret satellite-derived LAI should take seasonal dynamics of vegetation phenology into account, especially during periods of rapid green-up or peak growth [91–93]. Taken together, these results indicate that MODIS LAI likely represents an upper bound on canopy density in the Piedmont Grasslands during peak growing conditions and should be interpreted cautiously in assessing recovery and modeling ecosystem processes.

3.3. Uncertainty in measurements and observations of LAI

Uncertainty in ΔLAI (the difference between satellite and ground measurements) tends to be smallest during spring and largest during summer (figure 5). As compared to ground observations, MODIS overestimates summer LAI for Coastal Savannas and underestimates it the Piedmont Grasslands (figure 5(a)). While the spread in MODIS ΔLAI is large for both savannas and grasslands, their uncertainty ranges (mean ± 1 standard deviation) hardly overlap after May, indicating ecoregion specific variation. Shaded regions of ΔLAI are mostly negative after May for Piedmont Grasslands and positive for Coastal Savannas. In contrast, Landsat shows similar uncertainties for summer LAI for all ecoregions, but underestimates autumn LAI in grasslands with larger standard deviations (figure 5 (b)). With fewer data points (some months only having one), Piedmont Forest ΔLAI values are closer to zero and tend to fall within the bounds of the Coastal Savannas and Piedmont Grasslands. The smaller ΔLAI uncertainty

ranges for Landsat likely reflect reduced variability within the finer Landsat pixels relative to the coarser MODIS pixels.

Interpretation of ΔLAI should account for the uncertainty in the inherent difference between ground-based measurements and satellite observations. Satellite-derived LAI is strongly linked to vegetation greenness [4], while the gap-fraction approach from the ground-based estimates captures vegetation density regardless of spectral reflectance. Despite being less green, or even brown, during the autumn and winter, grasses remain 'dense' as seen by the LI-COR estimates, explaining some of the negative bias in grasslands during these seasons. Finally, the LAI-2200 C averages over a footprint that expands with canopy height causing the representativeness to vary across landscapes [59]. Stand homogeneity and additional samples help reduce uncertainty; however, these differences should still be taken into account when comparing point-level measurements with pixel-sized observations to analyze vegetation structure and recovery.

3.4. Implications of variability in LAI for land managers and ecosystem modelers

Estimates of vegetation density play a critical role in understanding ecosystem function, managing fire risk, and modeling land-atmosphere interactions. The variability among post-fire vegetation phenology measurements has major implications for both land managers and ecosystem modelers. The following sections examine limitations in satellite detection, consequences for ecosystem modeling, and the need for improved ground validation in fire-adapted systems.

3.4.1. Detection of low intensity fire damage to vegetation by satellites

MODIS detected declines in LAI after the GS wildfire and logging at GR-Main, but detecting vegetation losses after prescribed fires is difficult due to rapid regrowth. Additional sources are often needed to identify fire events, including burn reports and database records [94, 95]. Data from national agencies like the Fire Information for Resource Management System (which uses moderate resolution satellite data [96, 97]) and Monitoring Trends in Burn Severity (MTBS, which relies on surface reflectances from Landsat [98]) can miss fires and underestimate burned area by more than 200% [99]. Furthermore, MTBS only tracks large fires greater than 500 acres (approximately 200 hectares) in the eastern US, so no fires in this study were recorded, though larger prescribed fires could be detected. From 2021 to 2024, MTBS recorded 32 prescribed fires, totaling 16 000 ha across NC [100]. In contrast, the NCWRC reported over 1600 prescribed fires covering over 70 000 ha in the same time period [101], and The Nature Conservancy of NC burns over 16 000 ha in the state annually [102]. Combined, these figures suggest far more burned area in NC than satellite-based national agencies report [103], consistent with other findings in the region [29]. More accurate records of burned area might come from regional databases like Southeast Prescribed Fire Permit Database [95] or the Southeast FireMap [104], but those records are not specifically tracking pre- and post-fire vegetation density which may be useful for ecosystem modelers. Accordingly, our data offer complimentary measurements to accompany other database and remote sensing observations enhancing our overall ability to assess post-fire vegetation regrowth dynamics and highlighting observational limitations for modeling post-fire vegetation dynamics and land atmosphere interactions.

3.4.2. Post-fire phenology and carbon and water cycling

Satellite derived estimates of LAI influence predictions of carbon and water fluctuations used in land-surface models and remote sensing algorithms [19, 91, 92, 105]. The Southeastern US comprises a substantial portion of the nation's fire-adapted landscapes [94], and the region plays an important role as a global carbon sink [106], which may be vulnerable to changing fire regimes [3, 24]. Overestimating LAI could inflate rates of carbon assimilation and evapotranspiration [70, 107], and vice-versa. Such biases, or uncertainties, can propagate through Earth system models, distorting assessments of vegetation productivity, water-use, and land-atmosphere feedbacks [108, 109]. The findings from this study can help guide the development of empirical relationships between ground observations and remote sensing, allowing for adjustments to LAI algorithms that account for seasonal dynamics and ecosystem-specific characteristics at improved spatiotemporal resolutions [110]. Developing ecosystem-dependent scale factors has been shown to improve estimates of near surface atmospheric aridity at local scales [111]. A similar approach can be implemented to improve or place bounds on LAI estimates, which in turn enhances the accuracy of carbon assimilation, evapotranspiration, and water flux simulations in Earth system models. Such adjustments will improve the reliability of satellite LAI products for use in Earth system models that simulate vegetation carbon uptake and water fluxes.

3.4.3. Need for ground validation in fire-adapted ecosystems

Discrepancies between ground-based and remotely sensed observations of canopy density also have important implications for land managers, particularly in estimating fuel loads [112, 113] which are critical for predicting fire behavior during prescribed burn planning [114]. When land managers are estimating fuel loads, they will want to consider dead vegetation density (i.e. LICOR observations) rather than estimates based on greenness (i.e. satellite remote sensing methods). Improving understanding of post-fire vegetation regrowth dynamics is essential, particularly through ground-validation campaigns that can better inform widely-used remote sensing measurements. The fire monitoring community can use these results to inform dataset selection when using rapid changes in vegetation to detect fire events [99]. Though grounded in NC, our results highlight broader challenges and opportunities for using satellite-based vegetation monitoring in fire-adapted ecosystems worldwide [115].

4. Conclusion

Using ground and satellite-derived LAI from MODIS and Landsat, we demonstrated rapid post-fire vegetation regrowth across NC ecoregions and identified sources of uncertainty that vary by region and season, including land cover misclassifications, sub-pixel heterogeneity, and sensor variability. These findings have implications beyond the study region and demonstrate the utility of ground-based campaigns across diverse ecoregions to better characterize uncertainty in satellite monitoring of fire-affected regions. Future research should develop empirical relationships between ground observations and remote sensing to scale uncertainty assessments across larger burned areas [48], accounting for seasonal variations in vegetation phenology that may influence discrepancies between ground and remotely-sensed measurements of LAI. Biases in estimates of post-fire LAI propagate to carbon, water, and energy exchanges. Misinterpreting the rate or extent of regrowth could lead to incorrectly assessing ecosystem recovery and post-fire carbon assimilation. Additionally, land managers who use vegetation indices to guide prescribed fire planning should consider uncertainties in post-fire regrowth and vegetation density, as these affect fuel load estimates and the timing of future burns.

Acknowledgments

We would like to acknowledge our partners in fire for providing descriptions of vegetation land cover at each of the study sites, for granting us access to managed lands for data collection, and allowing our presence on days of prescribed burning: Wake Forest University Reynolda Gardens, Ruth Ann and Amy Grissom, The Nature Conservancy of North Carolina Coastal Plains, the North Carolina Wildlife Resources Commission, and the North Carolina Forest Service. A special thanks goes to Matthew Barnes, undergraduate student in the Lowman Lab, who conducted preliminary work in extracting LAI from Landsat in Google Earth Engine. Thank you David Carchipulla-Morales, PhD student in the Lowman Lab, for scouting sites with N Corak at the coast and for helping with the analyses in Google Earth Engine. Thank you to Z Carter Berry for helping the Lowman Lab with preliminary field campaigns, and to all of the undergraduates in the Lowman Lab who accompanied N Corak throughout the four years. And a token of gratitude goes to Jeff Wilcox who helped expand this work to the mountains of North Carolina. N Corak was supported by the 2024-2025 NC Space Grant Graduate Research Fellowship and the joint 2022-2023 NC Sea Grant—NC Space Grant Graduate Research Fellowship. This research was made possible by the Pilot Research Grant from the WFU Office of Research and Sponsored Programs and was supported in part by National Science Foundation (NSF) award AccelNet-Design: iFireNet: An international network of networks for prediction and management of wildland fires under Grant No. 2114740 for L E L Lowman.

Data availability statement

The data that support the findings of this study will be openly available following an embargo at the following URL/DOI: https://github.com/nick-corak/NC_PrescribedFires_LAI [116]. Data will be available from 01 July 2026.

Conflict of interest

The authors report no conflict of interest.

Author contributions

N K Corak 0000-0001-8452-4802
Conceptualization (equal), Data curation (equal), Formal analysis (lead), Funding acquisition (equal), Investigation (equal), Methodology (equal), Project administration (equal), Supervision (equal), Validation (equal), Visualization (equal), Writing – original draft (lead), Writing – review & editing (equal)

S J Kim-Shapiro 0009-0002-6738-7134
Data curation (equal), Formal analysis (supporting), Methodology (equal), Validation (supporting), Visualization (supporting), Writing – original draft (supporting), Writing – review & editing (supporting)

K T Chiarieri
Formal analysis (supporting), Investigation (supporting), Methodology (supporting), Visualization (equal), Writing – review & editing (supporting)

L E L Lowman 0000-0003-2960-7095
Conceptualization (lead), Formal analysis (equal), Funding acquisition (equal), Investigation (equal), Methodology (equal), Project administration (equal), Resources (equal), Supervision (lead), Writing – original draft (equal), Writing – review & editing (equal)

References

[1] Friedlingstein P *et al* 2025 Global carbon budget 2024 *Earth Syst. Sci. Data* **17** 965–1039
[2] Bowman D M J S, Kolden C A, Abatzoglou J T, Johnston F H, van der Werf G R and Flannigan M 2020 Vegetation fires in the anthropocene *Nat. Rev. Earth Environ.* **1** 500–15
[3] Abatzoglou J T and Williams A P 2016 Impact of anthropogenic climate change on wildfire across western us forests *Proc. Natl Acad. Sci.* **113** 11770–5
[4] Myneni R B *et al* 2002 Global products of vegetation leaf area and fraction absorbed PAR from year one of MODIS data *Remote Sens. Environ.* **83** 214–31
[5] Fang H, Baret F, Plummer S and Schaepman-Strub G 2019 An overview of global leaf area index (LAI): methods, products, validation and applications *Rev. Geophys.* **57** 739–99
[6] Monteith J and Unsworth M 2013 *Principles of Environmental Physics: Plants, Animals and the Atmosphere* (Academic)
[7] Baret F, Weiss M, Lacaze R, Camacho F, Makhmara H, Pacholcyzk P and Smets B 2013 GEOV1: LAI and FAPAR essential climate variables and FCOVER global time series capitalizing over existing products. Part1: principles of development and production *Remote Sens. Environ.* **137** 299–309
[8] McMichael C E, Hope A S, Roberts D A and Anaya M R 2004 Post-fire recovery of leaf area index in california chaparral: a remote sensing-chronosequence approach *Int. J. Remote Sens.* **25** 4743–60
[9] Boer M M, Macfarlane C, Norris J, Sadler R J, Wallace J and Grierson P F 2008 Mapping burned areas and burn severity patterns in SW Australian eucalypt forest using remotely-sensed changes in leaf area index *Remote Sens. Environ.* **112** 4358–69
[10] Wu J and Liang S 2020 Assessing terrestrial ecosystem resilience using satellite leaf area index *Remote Sens.* **12** 595
[11] Remke M, Schneider K and Korb J 2025 Leafing out: leaf area index as an indicator for mountain forest recovery following mixed-severity wildfire in southwest colorado *Forests* **16** 872
[12] Fang H, Wei S and Liang S 2012 Validation of MODIS and cyclopes LAI products using global field measurement data *Remote Sens. Environ.* **119** 43–54
[13] Alton P B 2016 The sensitivity of models of gross primary productivity to meteorological and leaf area forcing: a comparison between a penman–monteith ecophysiological approach and the MODIS light-use efficiency algorithm *Agric. Forest Meteorol.* **218** 11–24
[14] Boussetta S, Balsamo G, Beljaars A, Kral T and Jarlan L 2013 Impact of a satellite-derived leaf area index monthly climatology in a global numerical weather prediction model *Int. J. Remote Sens.* **34** 3520–42
[15] Boussetta S, Balsamo G, Dutra E, Beljaars A and Albergel C 2015 Assimilation of surface albedo and vegetation states from satellite observations and their impact on numerical weather prediction *Remote Sens. Environ.* **163** 111–26
[16] Zhuo W, Fang S, Gao X, Wang L, Wu D, Fu S, Wu Q and Huang J 2022 Crop yield prediction using MODIS LAI, TIGGE weather forecasts and WOFOST model: a case study for winter wheat in Hebei, China during 2009–2013 *Int. J. Appl. Earth Obs. Geoinf.* **106** 102668
[17] Doraiswamy P C, Moulin S, Cook P W and Stern A 2003 Crop yield assessment from remote sensing *Photogramm. Eng. Remote Sens.* **69** 665–74
[18] Doraiswamy P C, Hatfield J L, Jackson T J, Akhmedov B, Prueger J and Stern A 2004 Crop condition and yield simulations using Landsat and MODIS *Remote Sens. Environ.* **92** 548–59
[19] Bonan G B 1993 Importance of leaf area index and forest type when estimating photosynthesis in boreal forests *Remote Sens. Environ.* **43** 303–14

[20] Bonan G B 2008 Forests and climate change: forcings, feedbacks and the climate benefits of forests *Science* **320** 1444–9
[21] Hallema D W, Sun G, Caldwell P V, Norman S P, Cohen E C, Liu Y, Bladon K D and McNulty S G 2018 Burned forests impact water supplies *Nat. Commun.* **9** 1307
[22] Fisher J L, Loneragan W A, Dixon K, Delaney J and Veneklaas E J 2009 Altered vegetation structure and composition linked to fire frequency and plant invasion in a biodiverse woodland *Biol. Conserv.* **142** 2270–81
[23] Bowman D M J S *et al* 2009 Fire in the earth system *Science* **324** 481–4
[24] Mitchell R J, Liu Y, O'Brien J J, Elliott K J, Starr G, Miniat C F and Hiers J K 2014 Future climate and fire interactions in the southeastern region of the united states *For. Ecol. Manage.* **327** 316–26
[25] Collins S L and Calabrese L B 2012 Effects of fire, grazing and topographic variation on vegetation structure in tallgrass prairie *J. Vegetation Sci.* **23** 563–75
[26] Pausas J G and Keeley J E 2009 A burning story: the role of fire in the history of life *BioScience* **59** 593–601
[27] Fowler C and Konopik E 2007 The history of fire in the southern united states *Hum. Ecol. Rev.* **14** 165–76 (available at: www.jstor.org/stable/24707703)
[28] Jose S, Jokela E J and Miller D L 2006 *The Longleaf Pine Ecosystem: Ecology, Silviculture, and Restoration* (*Springer Series on Environmental Management*) (Springer)
[29] Nowell H K, Holmes C D, Robertson K, Teske C and Hiers J K 2018 A new picture of fire extent, variability and drought interaction in prescribed fire landscapes: insights from florida government records *Geophys. Res. Lett.* **45** 7874–84
[30] Simha A and Wright J P 2025 Short-term prescribed fire frequency manipulation alters community response to subsequent fires in a southeastern pine savanna *J. Ecol.* **113** 701–12
[31] Jones M W *et al* 2022 Global and regional trends and drivers of fire under climate change *Rev. Geophys.* **60** e2020RG000726
[32] Han A, Qing S, Bao Y, Na Li, Bao Y, Liu X, Zhang J and Wang C 2021 Short-term effects of fire severity on vegetation based on sentinel-2 satellite data *Sustainability* **13** 432
[33] Roberts G, Wooster M J, Lauret N, Gastellu-Etchegorry J-P, Lynham T and McRae D 2018 Investigating the impact of overlying vegetation canopy structures on fire radiative power (FRP) retrieval through simulation and measurement *Remote Sens. Environ.* **217** 158–71
[34] Pérez-Cabello F, Montorio R and Alves D B 2021 Remote sensing techniques to assess post-fire vegetation recovery *Curr. Opin. Environ. Sci. Health* **21** 100251
[35] Chu T, Guo X and Takeda K 2016 Remote sensing approach to detect post-fire vegetation regrowth in Siberian boreal larch forest *Ecol. Indicators* **62** 32–46
[36] Kibler C L, Parkinson A-M L, Peterson S H, Roberts D A, D'Antonio C M, Meerdink S K and Sweeney S H 2019 Monitoring post-fire recovery of chaparral and conifer species using field surveys and landsat time series *Remote Sens.* **11** 2963
[37] Helman D 2018 Land surface phenology: what do we really 'see' from space? *Sci. Total Environ.* **618** 665–73
[38] Huete A, Didan K, Miura T, Rodriguez E P, Gao X and Ferreira L G 2002 Overview of the radiometric and biophysical performance of the MODIS vegetation indices *Remote Sens. Environ.* **83** 195–213
[39] Van Leeuwen W J D 2008 Monitoring the effects of forest restoration treatments on post-fire vegetation recovery with MODIS multitemporal data *Sensors* **8** 2017–42
[40] Lacouture D L, Broadbent E N and Crandall R M 2020 Detecting vegetation recovery after fire in a fire-frequented habitat using normalized difference vegetation index (NDVI) *Forests* **11** 749
[41] Lentile L B, Holden Z A, Smith A M S, Falkowski M J, Hudak A T, Morgan P, Lewis S A, Gessler P E and Benson N C 2006 Remote sensing techniques to assess active fire characteristics and post-fire effects *Int. J. Wildland Fire* **15** 319–45
[42] Flerchinger G N, Seyfried M S and Hardegree S P 2016 Hydrologic response and recovery to prescribed fire and vegetation removal in a small rangeland catchment *Ecohydrology* **9** 1604–19
[43] Gričar J, Hafner P, Lavrič M, Ferlan M, Ogrinc N, Krajnc B, Eler K and Vodnik D 2020 Post-fire effects on development of leaves and secondary vascular tissues in Quercus pubescens *Tree Physiol.* **40** 796–809
[44] Li X, Kimball S, Ta P, Schmidt K T and Campbell D R 2024 Understanding post-fire vegetation recovery in southern california ecosystems with the aid of pre-fire observations from long-term monitoring *J. Vegetation Sci.* **35** e13308
[45] Wilson J W 1963 Estimation of foliage denseness and foliage angle by inclined point quadrats *Aust. J. Bot.* **11** 95–105
[46] MacArthur R H and Horn H S 1969 Foliage profile by vertical measurements *Ecology* **50** 802–4
[47] Welles J M and Norman J M 1991 Instrumentation for indirect measurement of canopy architecture *Agron. J.* **83** 818–25
[48] Woodgate W, Jones S D, Suarez L, Hill M J, Armston J D, Wilkes P, Soto-Berelov M, Haywood A and Mellor A 2015 Understanding the variability in ground-based methods for retrieving canopy openness, gap fraction and leaf area index in diverse forest systems *Agric. For. Meteorol.* **205** 83–95
[49] Ryan K C, Knapp E E and Varner J M 2013 Prescribed fire in north american forests and woodlands: history, current practice and challenges *Front. Ecol. Environ.* **11** e15–e24
[50] Elliott K J, Hendrick R L, Major A E, Vose J M and Swank W T 1999 Vegetation dynamics after a prescribed fire in the southern appalachians *For. Ecol. Manage.* **114** 199–213
[51] Cook C L, Bourgeau-Chavez L, Bilt D V, Miller M E, Kraatz S, Cosh M H, Kelly V R and Colliander A 2025 Comparison of *insitu* plant area index and remotely sensed leaf area index of northeastern american deciduous, mixed and coniferous forests for smapvex19-22 *IEEE J. Sel. Top. Appl. Earth Obs. Remote Sens.* **18** 18251–63
[52] Shabanov N V, Wang Y, Buermann W, Dong J, Hoffman S, Smith G R, Tian Y, Knyazikhin Y and Myneni R B 2003 Effect of foliage spatial heterogeneity in the MODIS LAI and FPAR algorithm over broadleaf forests *Remote Sens. Environ.* **85** 410–23
[53] Harley G L *et al* 2023 The longleaf tree-ring network: reviewing and expanding the utility of pinus palustris Mill. dendrochronological data *Prog. Phys. Geogr. Earth Environ.* **47** 570–96
[54] Soulé P T, Knapp P A, Maxwell J T and Mitchell T J 2021 A comparison of the climate response of longleaf pine (Pinus palustris Mill.) trees among standardized measures of earlywood, latewood, adjusted latewood and totalwood radial growth *Trees* **35** 1065–74
[55] Patterson T W and Knapp P A 2016 Stand dynamics influence masting/radial growth relationships in pinus palustris mill *Castanea* **81** 314–22
[56] Bucher M A and High M E 2002 Fire management and research for biodiversity in the green swamp *Proceedings: The Role of Fire for Nongame Wildlife Management and Community Restoration: Traditional Uses and New Directions* ed W M Ford, K R Russell and C E Moorman (U.S. Department of Agriculture, Forest Service, Northeastern Research Station) pp 111–4
[57] Monsi M and Saeki T 2005 On the factor light in plant communities and its importance for matter production *Ann. Bot.* **95** 549–67

[58] Bréda N J J 2003 Ground-based measurements of leaf area index: a review of methods, instruments and current controversies *J. Exp. Bot.* **54** 2403–17
[59] LI-COR Biosciences 2017 LAI-2200C plant canopy analyzer instruction manual LI-COR Biosciences Version 2200C-12027-20 (available at: www.licor.com/env/support/LAI-2200C/manuals.html)
[60] Myneni R, Knyazikhin Y and Park T 2021 MODIS/Terra Leaf Area Index/FPAR 8-Day L4 Global 500m SIN Grid V061 [Data set] (Accessed 24 March 2025)
[61] Knyazikhin Y et al 1999 MODIS Leaf Area Index (LAI) and Fraction of Photosynthetically Active Radiation Absorbed by Vegetation (FPAR) product (MOD15) algorithm theoretical basis document. *Technical Report* (NASA EOS Project Science Office)
[62] Friedl M A *et al* 2002 Global land cover mapping from MODIS: algorithms and early results *Remote Sens. Environ.* **83** 287–302
[63] Kang Y, Ozdogan M, Gao F, Anderson M C, White W A, Yang Y, Yang Y and Erickson T A 2021 A data-driven approach to estimate leaf area index for landsat images over the contiguous US *Remote Sens. Environ.* **258** 112383
[64] Gorelick N, Hancher M, Dixon M, Ilyushchenko S, Thau D and Moore R 2017 Google earth engine: planetary-scale geospatial analysis for everyone *Remote Sens. Environ.* **202** 18–27
[65] Roy D P *et al* 2014 Landsat-8: science and product vision for terrestrial global change research *Remote Sens. Environ.* **145** 154–72
[66] Yang L *et al* 2018 A new generation of the united states national land cover database: requirements, research priorities, design and implementation strategies *ISPRS J. Photogramm. Remote Sens.* **146** 108–23
[67] Dewitz J 2023 National land cover database (NLCD) 2021 products (U.S. Geological Survey)
[68] Savitzky A and Golay M J E 1964 Smoothing and differentiation of data by simplified least squares procedures *Anal. Chem.* **36** 1627–39
[69] Chen J, Jönsson P, Tamura M, Gu Z, Matsushita B and Eklundh L 2004 A simple method for reconstructing a high-quality ndvi time-series data set based on the Savitzky–Golay filter *Remote Sens. Environ.* **91** 332–44
[70] Yang W, Huang D, Tan B, Stroeve J C, Shabanov N V, Knyazikhin Y, Nemani R R and Myneni R B 2006 Analysis of leaf area index and fraction of PAR absorbed by vegetation products from the terra MODIS sensor: 2000–2005 *IEEE Trans. Geosci. Remote Sens.* **44** 1829–42
[71] Corak N K, Otkin J A, Ford T W and Lowman L E L 2024 Unraveling phenological and stomatal responses to flash drought and implications for water and carbon budgets *Hydrol. Earth Syst. Sci.* **28** 1827–51
[72] Lowman L E L, Christian J I and Hunt E D 2023 How land surface characteristics influence the development of flash drought through the drivers of soil moisture and vapor pressure deficit *J. Hydrometeorol.* **24** 1395–415
[73] Garrigues S, Allard D, Baret F'eric and Weiss M 2006 Influence of landscape spatial heterogeneity on the non-linear estimation of leaf area index from moderate spatial resolution remote sensing data *Remote Sens. Environ.* **105** 286–98
[74] Xu D, An D and Guo X 2020 The impact of non-photosynthetic vegetation on LAI estimation by NDVI in mixed grassland *Remote Sens.* **12** 1979
[75] Welles J M and Cohen S 1996 Canopy structure measurement by GAP fraction analysis using commercial instrumentation *J. Exp. Bot.* **47** 1335–42
[76] Sprintsin M, Karnieli A, Berliner P, Rotenberg E, Yakir D and Cohen S 2009 Evaluating the performance of the MODIS leaf area index (LAI) product over a mediterranean dryland planted forest *Int. J. Remote Sens.* **30** 5061–9
[77] Fang H, Li W and Myneni R B 2013 The impact of potential land cover misclassification on MODIS leaf area index (LAI) estimation: a statistical perspective *Remote Sens.* **5** 830–44
[78] Peet M, Anderson R and Adams M S 1975 Effect of fire on big bluestem production *Am. Midland Nat.* **94** 15–26
[79] Ripley B, Donald G, Osborne C P, Abraham T and Martin T 2010 Experimental investigation of fire ecology in the C3 and C4 subspecies of alloteropsis semialata *J. Ecol.* **98** 1196–203
[80] Simpson K J, Jardine E C, Archibald S, Forrestel E J, Lehmann C E R, Thomas G H and Osborne C P 2021 Resprouting grasses are associated with less frequent fire than seeders *New Phytol.* **230** 832–44
[81] Ripley B, Visser V, Christin P-A, Archibald S, Martin T and Osborne C 2015 Fire ecology of C3 and C4 grasses depends on evolutionary history and frequency of burning but not photosynthetic type *Ecology* **96** 2679–91
[82] Yan K, Wang J, Peng R, Yang K, Chen X, Yin G, Dong J, Weiss M, Pu J and Myneni R B 2024 HiQ-LAI: a high-quality reprocessed MODIS leaf area index dataset with better spatiotemporal consistency from 2000 to 2022 *Earth Syst. Sci. Data* **16** 1601–22
[83] Stenberg P 1996 Correcting LAI-2000 estimates for the clumping of needles in shoots of conifers *Agric. Forest Meteorol.* **79** 1–8
[84] Garrigues S, Shabanov N V, Swanson K, Morisette J T, Baret F'eric and Myneni R B 2008 Intercomparison and sensitivity analysis of leaf area index retrievals from lai-2000, accupar and digital hemispherical photography over croplands *Agric. For. Meteorol.* **148** 1193–209
[85] Asrar G, Kanemasu E T, Miller G P and Weiser R L 1986 Light interception and leaf area estimates from measurements of grass canopy reflectance *IEEE Trans. Geosci. Remote Sens.* **GE-24** 76–82
[86] Drewa P B, Platt W J and Moser E B 2002 Fire effects on resprouting of shrubs in headwaters of southeastern longleaf pine savannas *Ecology* **83** 755–67
[87] Vose J M, Peterson D L, Fettig C J, Halofsky J E, Hiers J K, Keane R E, Loehman R and Stambaugh M C 2021 Fire and forests in the 21st century: managing resilience under changing climates and fire regimes in usa forests *Fire Ecology and Management: Past, Present and Future of US Forested Ecosystems* vol 39 pp 465–502 (Springer)
[88] Kupfer J A, Lackstrom K, Grego J M, Dow K, Terando A J and Hiers J K 2022 Prescribed fire in longleaf pine ecosystems: fire managers' perspectives on priorities, constraints and future prospects *Fire Ecol.* **18** 27
[89] Wright J K, Williams M, Starr G, Mcgee J and Mitchell R J 2013 Measured and modelled leaf and stand-scale productivity across a soil moisture gradient and a severe drought *Plant, Cell Environ.* **36** 467–83
[90] Ross C W, Loudermilk E L, O'Brien J J, Flanagan S A, McDaniel J, Aubrey D P, Lowe T, Hiers J K and Skowronski N S 2024 Lidar-derived estimates of For. structure in response to fire frequency *Fire Ecol.* **20** 44
[91] Running S W and Coughlan J C 1988 A general model of forest ecosystem processes for regional applications I. Hydrologic balance, canopy gas exchange and primary production processes *Ecol. Model.* **42** 125–54
[92] Baldocchi D D, Wilson K B and Gu L 2002 How the environment, canopy structure and canopy physiological functioning influence carbon, water and energy fluxes of a temperate broad-leaved deciduous forest-an assessment with the biophysical model CANOAK *Tree Physiol.* **22** 1065–77
[93] Anav A *et al* 2015 Spatiotemporal patterns of terrestrial gross primary production: a review *Rev. Geophys.* **53** 785–818
[94] Melvin M A. 2021 national prescribed fire use survey report *Technical Report* (National Association of State Foresters and the Coalition of Prescribed Fire Councils)

[95] Cummins K, Noble J, Varner J M, Robertson K M, Hiers J K, Nowell H K and Simonson E 2023 The southeastern us prescribed fire permit database: hot spots and hot moments in prescribed fire across the southeastern USA *Fire* **6** 372
[96] Giglio L, Schroeder W and Justice C O 2016 The collection 6 MODIS active fire detection algorithm and fire products *Remote Sens. Environ.* **178** 31–41
[97] Schroeder W, Oliva P, Giglio L and Csiszar I A 2014 The new VIIRS 375 m active fire detection data product: Algorithm description and initial assessment *Remote Sens. Environ.* **143** 85–96
[98] Eidenshink J, Schwind B, Brewer K, Zhu Z-L, Quayle B and Howard S 2007 A project for monitoring trends in burn severity *Fire Ecology* **3** 3–21
[99] Hawbaker T J *et al* 2017 Mapping burned areas using dense time-series of landsat data *Remote Sens. Environ.* **198** 504–22
[100] MTBS. Data access: fire level geospatial data 2017 *Monitoring Trends in Burn Severity Project* (USDA For. Service/U.S. Geological Survey) (available at: http://mtbs.gov/direct-download) (Accessed 14 June 2025)
[101] North Carolina Wildlife Resources Commission 2024 Prescribed fire dashboard (available at: www.arcgis.com/apps/dashboards/eb912135135c4a14b6bc088750570f76) (Accessed 14 June 2025)
[102] The Nature Conservancy 2025 The role of fire in forests (The Nature Conservancy) (available at: www.nature.org/en-us/about-us/where-we-work/united-states/north-carolina/stories-in-north-carolina/fire-forests/)
[103] Li F, Zhang X, Kondragunta S, Schmidt C C and Holmes C D 2020 A preliminary evaluation of GOES-16 active fire product using Landsat-8 and VIIRS active fire data and ground-based prescribed fire records *Remote Sens. Environ.* **237** 111600
[104] Teske C, Vanderhoof M K, Hawbaker T J, Noble J and Hiers J K 2021 Using the landsat burned area products to derive fire history relevant for fire management and conservation in the state of florida, southeastern USA *Fire* **4** 26
[105] Law B E *et al* 2002 Environmental controls over carbon dioxide and water vapor exchange of terrestrial vegetation *Agric. For. Meteorol.* **113** 97–120
[106] Lu X, Kicklighter D W, Melillo J M, Reilly J M and Xu L 2015 Land carbon sequestration within the conterminous united states: regional-and state-level analyses *J. Geophys. Res. Biogeosci.* **120** 379–98
[107] Xie X, Li A, Jin H, Tan J, Wang C, Lei G, Zhang Z, Bian J and Nan Xi 2019 Assessment of five satellite-derived LAI datasets for GPP estimations through ecosystem models *Sci. Total Environ.* **690** 1120–30
[108] Raupach M R, Rayner P J, Barrett D J, DeFries R S, Heimann M, Ojima D S, Quegan S and Schmullius C C 2005 Model–data synthesis in terrestrial carbon observation: methods, data requirements and data uncertainty specifications *Global Change Biol.* **11** 378–97
[109] Richardson A D *et al* 2010 Estimating parameters of a For. ecosystem C model with measurements of stocks and fluxes as joint constraints *Oecologia* **164** 25–40
[110] Li W, Weiss M, Buis S, Verger A, Jay S, Ren Z, Wu W, Jiang J, Comar A and De Solan B 2026 NRT-GSF: a novel near-real-time ground-satellite fusion algorithm to retrieve daily green area index at field scale *Remote Sens. Environ.* **333** 115160
[111] Corak N K, Thornton P E and Lowman L E L 2025 A high resolution, gridded product for vapor pressure deficit using daymet *Sci. Data* **12** 256
[112] Parresol B R, Blake J I and Thompson A J 2012 Effects of overstory composition and prescribed fire on fuel loading across a heterogeneous managed landscape in the southeastern USA *For. Ecol. Manage.* **273** 29–42
[113] Gale M G, Cary G J, Van Dijk A I J M and Yebra M 2021 Forest fire fuel through the lens of remote sensing: review of approaches, challenges and future directions in the remote sensing of biotic determinants of fire behaviour *Remote Sens. Environ.* **255** 112282
[114] Arroyo L A, Pascual C and Manzanera J A 2008 Fire models and methods to map fuel types: the role of remote sensing *For. Ecol. Manage.* **256** 1239–52
[115] Simpson K J, Archibald S and Osborne C P 2022 Savanna fire regimes depend on grass trait diversity *Trends Ecol. Evol.* **37** 749–58
[116] Corak N K, Kim-Shapiro S J, Chiarieri K T and Lowman L E L, 2025 NC_PrescribedFires_LAI *Github* (available at: https://github.com/nick-corak/NC_PrescribedFires_LAI)